

CSE1L, a Novel Microvesicle Membrane Protein, Mediates Ras-Triggered Microvesicle Generation and Metastasis of Tumor Cells

Ching-Fong Liao,^{1*} Shu-Hui Lin,^{2,3*} Hung-Chang Chen,⁴ Cheng-Jeng Tai,^{5,6} Chun-Chao Chang,^{5,7} Li-Tzu Li,¹ Chung-Min Yeh,^{2,3} Kun-Tu Yeh,^{2,8,9} Ying-Chun Chen,¹ Tsu-Han Hsu,¹ Shing-Chuan Shen,¹⁰ Woan-Ruoh Lee,¹⁰ Jeng-Fong Chiou,¹¹ Shue-Fen Luo,¹² and Ming-Chung Jiang⁵

¹Institute of Cellular and Organismic Biology, Academia Sinica, Taipei, Taiwan; ²Department of Pathology, Changhua Christian Hospital, Changhua, Taiwan; ³Department of Medical Technology, Jen-Teh Junior College of Medicine, Nursing and Management, Miaoli, Taiwan; ⁴Division of Colorectal Surgery, Changhua Christian Hospital, Changhua, Taiwan; ⁵Department of Internal Medicine, School of Medicine, College of Medicine, Taipei Medical University, Taipei, Taiwan; ⁶Division of Hematology and Oncology, Department of Internal Medicine, Taipei Medical University Hospital, Taipei, Taiwan; ⁷Division of Gastroenterology and Hepatology, Department of Internal Medicine, Taipei Medical University Hospital, Taipei, Taiwan; ⁸School of Medicine, Chung Shan Medical University, Taichung, Taiwan; ⁹Institute of Clinical Medicine, Kaohsiung Medical University, Kaohsiung, Taiwan; ¹⁰Graduate Institute of Medical Sciences, College of Medicine, Taipei Medical University, Taipei, Taiwan; ¹¹Department of Radiation Oncology, School of Medicine, College of Medicine, Taipei Medical University, Taipei, Taiwan; and ¹²Department of Medicine, Division of Allergy, Immunology and Rheumatology, Chang Gung Memorial Hospital, Chang Gung University College of Medicine, Tao-yuan, Taiwan

Tumor-derived microvesicles are rich in metastasis-related proteases and play a role in the interactions between tumor cells and tumor microenvironment in tumor metastasis. Because shed microvesicles may remain in the extracellular environment around tumor cells, the microvesicle membrane protein may be the potential target for cancer therapy. Here we report that chromosome segregation 1-like (CSE1L) protein is a microvesicle membrane protein and is a potential target for cancer therapy. v-H-Ras expression induced extracellular signal-regulated kinase (ERK)-dependent CSE1L phosphorylation and microvesicle biogenesis in various cancer cells. CSE1L overexpression also triggered microvesicle generation, and CSE1L knockdown diminished v-H-Ras-induced microvesicle generation, matrix metalloproteinase (MMP)-2 and MMP-9 secretion and metastasis of B16F10 melanoma cells. CSE1L was preferentially accumulated in microvesicles and was located in the microvesicle membrane. Furthermore, anti-CSE1L antibody-conjugated quantum dots could target tumors in animal models. Our findings highlight a novel role of Ras-ERK signaling in tumor progression and suggest that CSE1L may be involved in the "early" and "late" metastasis of tumor cells in tumorigenesis. Furthermore, the novel microvesicle membrane protein, CSE1L, may have clinical utility in cancer diagnosis and targeted cancer therapy.

Online address: <http://www.molmed.org>

doi: 10.2119/molmed.2012.00205

INTRODUCTION

Microvesicles (microparticles) are plasma membrane-derived particles that are released from cells by the outward budding and fission of the plasma mem-

brane (1). Microvesicles play essential physiological/pathological roles, including the progression of the tumor via the modulation of tumor-stroma interactions, immune suppression, angiogenesis

and tumor metastasis (2–6). The interactions between neoplastic cells and their microenvironment components such as stroma, extracellular matrix and endothelial/inflammatory cells reside in the tumor microenvironment have great effects on tumor expansion and metastasis (7). Tumor cells constitutionally release microvesicles by the way they transmit their membrane growth factor receptors, metastasis-related proteases and other bioactive molecules to other tumor cells, nontumor cells and other tissue components in the tumor microenvironment, thereby promoting tumor progression (8, 9). It has been reported that

*C-FL and S-HL contributed equally to this work.

Address correspondence to Ming-Chung Jiang, Department of Internal Medicine, Taipei Medical University Hospital, Number 252 Wu-Hsing Street, Taipei 11031, Taiwan. Phone: +886-2-27372181; Fax: +886-2-27363051; E-mail: jiangmwd@gmail.com.

Submitted May 8, 2012; Accepted for publication August 28, 2012; Epub (www.molmed.org) ahead of print August 29, 2012.

microvesicle shedding is a major secretory pathway for cathepsin B, a metastasis-related protease, releasing from tumor cells (10). Studies with human and murine lung cancer cells have shown that microvesicles shed by tumor cells induce the expression of several pro-angiopoietic factors in stromal cells, thus actively modulating the behavior of endothelium and tumor stroma (11). Tumor-derived microvesicles are rich in metastasis-related proteases such as matrix metalloproteinase (MMP)-2 and MMP-9, which are involved in the degradation of extracellular matrix in the tumor microenvironment, thereby promoting tumor metastasis (12). The amounts of microvesicles shed by tumor cells have been reported to be correlated with the invasiveness of tumor cells both *in vitro* and *in vivo* (13). Thus, an understanding of the mechanism of microvesicle biogenesis can facilitate the control of cancer progression.

The *ras* family consists of three functional genes, *H-ras*, *K-ras* and *N-ras*, which encode highly similar 21-kDa Ras proteins. Mutations in codon 12, 13 or 61 of one of the three *ras* genes convert these genes into active oncogenes and activate the mitogen-activated protein kinase signaling and stimulate cancer progression (14). Ras is associated with both the initiation and malignant progression of the tumor (15). Aberrant activation of Ras was implicated in the metastasis of the tumor (16). Extracellular signal-regulated kinase (ERK) is a major downstream transducer of Ras (17). ERK has been shown to mediate the shedding of microvesicles during tumor invasion through the modulation of myosin light-chain kinase (MLCK) activation (18). Microvesicles need to be generated before being released outside the cell membrane. However, the cellular mechanism that regulates microvesicle biogenesis, therefore promoting tumor metastasis, is not fully understood.

The chromosome segregation 1-like (CSE1L) protein is the human homolog of CSE1, the yeast chromosome segregation protein (19). CSE1L is highly expressed in

cancer, and its expression is associated with advanced stage and poor outcome of cancer patients (20–28). CSE1L has been shown to regulate the migration of tumor cells (29). The shed microvesicles may remain in the extracellular environment around tumor cells; thus there may be a relatively higher level of microvesicles in the tumor microenvironment (4,30). Hence, microvesicle membrane proteins may be the potential targets for cancer therapy. We report here that CSE1L mediates microvesicle biogenesis. Furthermore, CSE1L is preferentially accumulated in microvesicles and is located in the microvesicle membrane. We show that anti-CSE1L antibody-conjugated quantum dots can target tumors in animal models. Our results suggest that CSE1L may be a potential target for targeted cancer therapy.

MATERIALS AND METHODS

Antibodies

The antibodies used in the experiment were anti-p21 / ras (EP1125Y) (Epitomics, Burlingame, CA, USA); anti-CSE1L (3D8) and anti-phospho-ERK1/2 (phospho T202/204, G15-B) (Abnova, Taipei, Taiwan); anti-phosphotyrosine (PY20) and anti-phosphoserine/threonine (22A/pSer/Thr) (BD Biosciences, San Jose, CA, USA); anti- β -tubulin (D66) (Sigma, St. Louis, MO, USA); anti- β -actin (Ab-5) and anti-GFP (Ab-1) (Lab Vision, Fremont, CA, USA); anti-CSE1L (24), anti-CSE1L (H2), anti-MMP-2 (H-76), anti-ERK1/2 (MK1) and anti-phosphothreonine (H2) (Santa Cruz Biotechnology, Santa Cruz, CA, USA); anti-MMP-9 (EP 1328Y) (Novus Biologicals, Littleton, CO, USA); goat anti-mouse IgG (Jackson Immuno-Research Laboratories, West Grove, PA, USA); and goat anti-mouse (or anti-rabbit) IgG secondary antibodies coupled with Alexa Fluor 488 (or 568) (Molecular Probes, Eugene, OR, USA).

Plasmids

v-H-Ras (pZIP-v-H-ras) expression vector carrying a neomycin selectable marker was provided by Channing J Der (31).

Mammalian CSE1L expression vector, pcDNA-CSE1L, carrying a neomycin selectable marker was generated by inserting *cse1l* complementary DNA (cDNA) as an *ApaI* and *NotI* fragment from the pGEM-CSE1L vector (29) into the *ApaI* and *NotI* sites of the pcDNA3.1 vector. The *cse1l* shRNA plasmids (sc-29909-SH) designed to knock down *cse1l* expression, and the control shRNA plasmids (sc-108060) encode of a scrambled shRNA sequence that will not lead to the specific degradation of any cellular any known cellular mRNA, were ordered from Santa Cruz Biotechnology. The shRNA plasmids carry the puromycin selectable marker.

Cells and DNA Transfections

B16F10 melanoma cells, Michigan Cancer Foundation-7 (MCF-7) breast cancer cells and HT-29 colon cancer cells were obtained from the American Type Culture Collection (Manassas, VA, USA). Cells were cultured in Dulbecco's modified Eagle's medium (DMEM) supplemented with 10% heat-inactivated fetal bovine serum (FBS), 100 units/mL penicillin, 100 mg/mL streptomycin and 2 mmol/L glutamate at 37°C under a humidified 5% CO₂ atmosphere. B16F10 cells were transfected with the control pZIP-NeoSV(X)1 empty vector (EV) plus control shRNA plasmids, pZIP-v-H-ras plus control shRNA plasmids, pcDNA-CSE1L plus control shRNA plasmids, and pZIP-v-H-ras plus *cse1l* shRNA plasmids to obtain B16-dEV, B16-Ras, B16-CSE1L and B16-Ras/anti-CSE1L cells, respectively, by using the Lipofectamine Plus reagent (Invitrogen, Carlsbad, CA, USA) according to the manufacturer's instructions. Transfected cells were selected with 1 mg/mL G418 for 3 wks and then with 1 μ g/mL puromycin for 3 wks. Multiple drug-resistant colonies (>50) were pooled together and amplified in mass culture. For the experiments, cells were cultured in medium without G418 and puromycin. In experiments where cells were treated with dimethyl sulfoxide (DMSO) or PD98059, the relative volume of solvent to total media was 5:10,000, and the concentra-

tion of PD98059 was 50 $\mu\text{mol/L}$ for all experiments.

Immunoblotting

Cells were washed with phosphate-buffered saline (PBS) and lysed in ice-cold radioimmunoprecipitation assay buffer (25 mmol/L Tris-HCl [pH 7.2], 0.1% sodium dodecyl sulfate [SDS], 0.1% Triton X-100, 1% sodium deoxycholate, 150 mmol/L NaCl, 1 mmol/L ethylenediaminetetraacetic acid [EDTA], 1 mmol/L sodium orthovanadate, 1 mmol/L phenylmethylsulfonyl fluoride, 10 $\mu\text{g/mL}$ aprotinin and 5 $\mu\text{g/mL}$ leupeptin). The protein concentrations were determined with a BCA protein assay kit (Pierce, Rockford, IL, USA). A total of 50 μg of each protein sample was loaded onto SDS-polyacrylamide gel. Proteins were transferred to nitrocellulose membranes (Amersham Pharmacia, Little Chalfont, Buckinghamshire, UK). The membrane was blocked at 4°C overnight in blocking buffer (1% bovine serum albumin [BSA], 50 mmol/L Tris-HCl [pH 7.6], 150 mmol/L NaCl and 0.1% Tween-20). The blots were incubated for 1 h at room temperature with primary antibodies followed by incubation with secondary antibodies conjugated to horseradish peroxidase for 1 h. The levels of protein were detected by enhanced chemiluminescence with a Forte Western HRP (horseradish peroxidase) Substrate (Millipore, Billerica, MA, USA). For immunoblotting with biotin-conjugated antibodies, the biotin-conjugated antibody was prepared by biotinylation anti-CSE1L antibodies by using the Biotin Labeling Kit-NH2 kit according to the manufacturer's protocol (Dojindo Laboratories, Kumamoto, Japan). The immunoblot reacted with HRP-conjugated streptavidin, and the levels of protein were detected by Forte Western HRP Substrate.

Immunofluorescence and Microvesicle Scoring

Cells grown on glass cover slides (12 \times 12 mm) for 4 d were changed to medium without FBS. After incubation for 24 h,

the cells were cytospun at 150g for 10 min. Cells were washed with PBS, fixed with 4% paraformaldehyde, permeabilized with methanol and blocked with PBS containing 0.1% BSA. Samples were incubated with primary antibodies for 1 h. Samples were then washed three times with PBS and followed by incubating with secondary antibodies coupled with Alexa Fluor 488 (or 568) and examined with an inverted fluorescence microscope. For each experimental condition, cells showing microvesicles at the surface were scored. A total of 300 cells were observed for each experiment, and the data from three independent experiments were plotted. Standard deviation bars are shown.

Conditioned Medium

Cells were grown to subconfluence, washed with PBS and changed to medium without FBS. After incubation for 24 h, the conditioned medium was collected, and the cell numbers were counted. To remove possible suspended cells or cell debris, medium was centrifuged at 10,000g for 10 min, after which the supernatant was harvested.

Cell Proliferation Assay

Equal numbers of cells (1×10^4 cells/dish) were seed on 100-mm culture dishes. The media were refreshed every 3 d. The cell numbers were counted every 24 h by trypan blue exclusion assays after cell seeding. For each time point, three plates of cells were counted, and each plate was only counted once.

Gelatin Zymography Assay

Microvesicles harvested from cell number-standardized conditioned media were resolved using 10% SDS-polyacrylamide gel electrophoresis (PAGE) containing 1 mg/mL gelatin. The gel was washed twice with 2.5% Triton X-100 for 30 min to remove SDS and was subsequently incubated in buffer containing 50 mmol/L Tris-HCl (pH 7.6), 200 mmol/L NaCl and 10 mmol/L CaCl_2 at 37°C for 24 h. The gel was stained with Coomassie blue R-250 (0.125% Co-

massie blue R-250, 50% methanol, 10% acetic acid) for 30 min and destained with destaining solution (20% methanol, 10% acetic acid, 70% deionized distilled water [ddH₂O]) until the clear bands were visualized.

Production of Glutathione S-transferase-CSE1L (GST-CSE1L) Fusion Protein

GST-CSE1L fusion protein was produced by using a wheat germ cell-free protein synthesis system according to the method described by ENDEXT technology protocol (CellFree Sciences, Yokohama, Japan). Briefly, the open reading frame of *cse1l* cDNA in the pcDNA-CSE1L vector was cut with restriction enzymes and was subcloned into the wheat germ expression vector pPEU-E01-MCS (CellFree Sciences). Transcription of *cse1l* mRNA was performed by adding 2 μg of the subcloned plasmid to a tube containing the transcription premixed solution (CellFree Sciences). The mixture was incubated at 37°C for 6 h for transcription reaction. A total of 10 μL of the mRNA mixture was added into 10 μL wheat germ extract solution (WEPRO 3240, CellFree Sciences) for translation reaction. The translation mixture (20 μL) was transferred to the bottom of the well containing SUB-AMIX (CellFree Sciences) to form a bilayer with the translation mixture in the lower layer. After incubated at 26°C for 16 h, the mixture was used to purify the GST-CSE1L fusion protein. GST-CSE1L fusion proteins were purified using glutathione-Sepharose 4B beads and Bulk GST Purification Modules (Amersham Pharmacia). The purified GST-CSE1L fusion protein was cleaved with thrombin, and GST was removed by using Amicon Ultra-4 Centrifugal Filter Units (Millipore).

Tissue Microarrays and Immunohistochemistry

Three tissue cores from colorectal cancer ($n = 115$), breast cancer ($n = 100$) and melanoma ($n = 92$), and one tissue core from noncancer tissue, in each paraffin block were longitudinally cut and ar-

ranged into new paraffin blocks by using the manual method of a Biosyn-Matric Handmade Kit (Formosa Transcrip Inc., Kaohsiung, Taiwan) to generate tissue microarrays. The tissue sections were stained with hematoxylin and eosin to confirm the presence of morphologically representative areas of the original cancers. For immunohistochemistry, the paraffin-embedded cancer specimens and paired nontumor tissue sections (4 μ m) were deparaffinized in xylene and rehydrated in graded alcohol. Antigen retrieval was performed by treatment with boiling citrate buffer (10 mmol/L, pH 6.0) for 20 min. Endogenous peroxidase activity was blocked with 3% hydrogen peroxide in water, and nonspecific staining was blocked by incubation with 5% BSA for 1 h at room temperature. After incubation with a 100-fold dilution of anti-CSE1L antibody (3D8, Abnova) for 20 min at room temperature and thorough washing three times with PBS, the slides were incubated with an HRP/Fab polymer conjugate for another 30 min. The sites of peroxidase activity were visualized by using diaminobenzidine (3,3'-diaminobenzidine tetrahydrochloride) as the substrate and counterstained with Mayer hematoxylin. In the negative control, the primary antibody was omitted and replaced by PBS.

Patients and Tumor Samples

Colorectal cancer samples were obtained from 115 consecutive patients who had been given a diagnosis at the Changhua Christian Hospital (Changhua, Taiwan). All participants had the study explained to them and gave informed consent by using institutional review board-approved guidelines before any participation. Serum samples were collected by allowing blood to sit at room temperature for a minimum of 30 min to allow clots to form. To remove any possible suspended cells or cell debris in serum, samples were centrifuged at 10,000g for 10 min, after which supernatants were harvested and stored at -80°C . Baseline characteristics of the pa-

tients are shown in Supplementary Table S1.

Immunoprecipitation

Cells grown on plastic dishes were washed with PBS and incubated in lysis buffer (10 mmol/L Tris-HCl [pH 7.4], 10 mmol/L EDTA, 0.4% deoxycholic acid, 1% Triton X-100, 1 mmol/L phenylmethylsulfonyl fluoride, 10 μ g/mL aprotinin and 5 μ g/mL leupeptin) at 4°C for 20 min. Cells were scraped and disrupted by pipetting. The cell lysate was cleared of insoluble materials by centrifugation at 10,000g for 10 min at 4°C , and the protein concentrations were determined with a BCA protein assay kit (Pierce). Equal amounts of cell lysate (500 μ g) isolated from B16-dEV and B16-CSE1L cells were

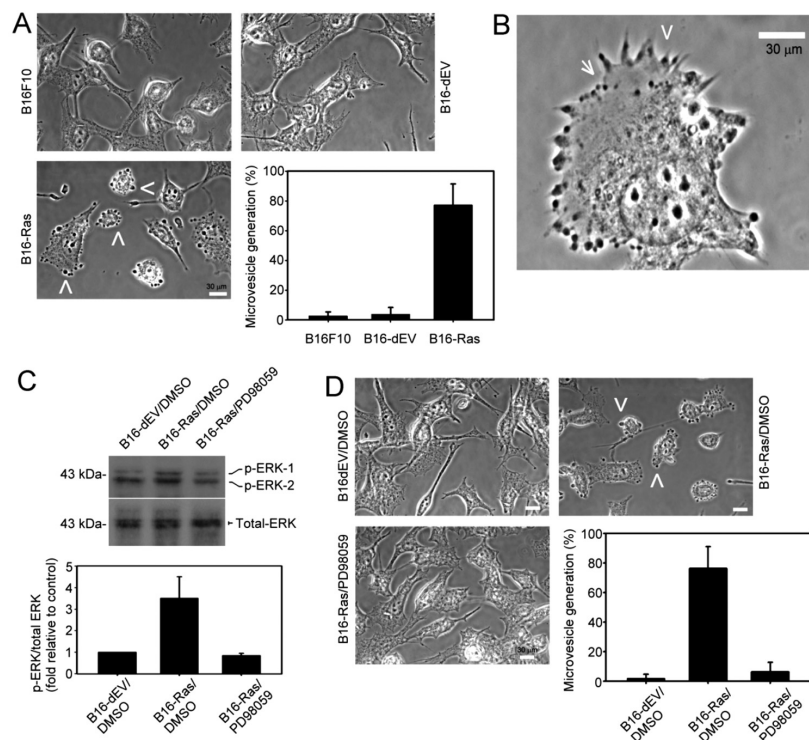


Figure 1. v-H-ras triggers microvesicle biogenesis. (A) Representative micrographs of B16F10, B16-dEV and B16-Ras cells. (B) Representative image shows the presence of developing microvesicles at the invadopodia (arrowhead) and the membrane (arrow) of B16-Ras cells. (C) Immunoblotting of phospho-ERK and total ERK in cell lysates from B16-dEV and B16-Ras cells treated with DMSO or PD98059 for 12 h. Band intensities were quantified by densitometry, and the ratio of phospho-ERK to total ERK is shown. (D) Representative micrographs of B16-dEV and B16-Ras cells treated with DMSO or PD98059 in medium without FBS for 12 h. Note that PD98059 treatment inhibited microvesicle biogenesis induced by v-H-ras.

separately incubated with immunoprecipitation buffer (50 mmol/L Tris-HCl [pH 7.5], 150 mmol/L NaCl and 0.25% gelatin) containing primary antibodies at 4°C for 3 h followed by a slurry of protein G plus/protein A-agarose (A/G plus agarose) beads (Santa Cruz Biotechnology) and incubated for an additional 2 h. The immunoprecipitates were washed with lysis buffer four times and then subjected to SDS-PAGE and immunoblotting with antibodies.

For immunoprecipitation with serum samples, sera were incubated at 4°C overnight in PBS containing agarose-conjugated anti-phosphothreonine antibodies (H2) (Santa Cruz Biotechnology), with slow rotation. The immunoprecipitates were washed with immunoprecipi-

tation lysis buffer three times and were then subjected to SDS-PAGE and immunoblotting with anti-CSE1L antibodies. Control immunoprecipitation was performed by using agarose-conjugated normal mouse IgG (Santa Cruz Biotechnology).

Matrigel-Based Invasion Assay

The Matrigel-based invasion assay was done using Matrigel (BD Biosciences) and 8- μm pore-sized polyvinylpyrrolidone-free polycarbonate filters (Costar, Cambridge, MA, USA). The filters were soaked in Matrigel diluted five-fold with DMEM. The filters were washed with DMEM and then were placed in microchemotaxis chambers. Cells were treated by 0.1% trypsin-EDTA digestion, resuspended in DMEM containing 10% FBS and then washed with serum-free DMEM. Cells (2×10^4) were finally suspended in DMEM (200 μL) and placed in the upper compartment of the chemotaxis chambers. Culture medium (300 μL) containing 20% FBS was placed in the lower compartment of the chemotaxis chambers to serve as a source of chemoattractants. After incubation for 6 h at 37°C, cells on the upper surface of the filters were completely wiped away with a cotton swab. Cells on the lower surface of the filters were fixed in methanol, stained with hematoxylin and eosin and then counted under a microscope. The assays were repeated three times, and each assay consisted of four replicates of filters. For each replicate, the migrated tumor cells in 10 randomly selected fields were determined, and the counts were averaged.

Animal Metastasis Models

Male C57BL/6 mice aged between 6 and 7 (n = 18) and 14 and 15 (n = 26) wks old (National Laboratory Animal Center, Taipei, Taiwan) were housed in an animal holding room under standard conditions (22°C; 50% humidity; 12-h light/dark cycle). The experiments included four groups (that is, mice injected with B16-dEV, B16-CSE1L, B16-Ras and B16-Ras/anti-CSE1L cells), and mice with different ages were evenly distributed in the four groups. Each mouse was in-

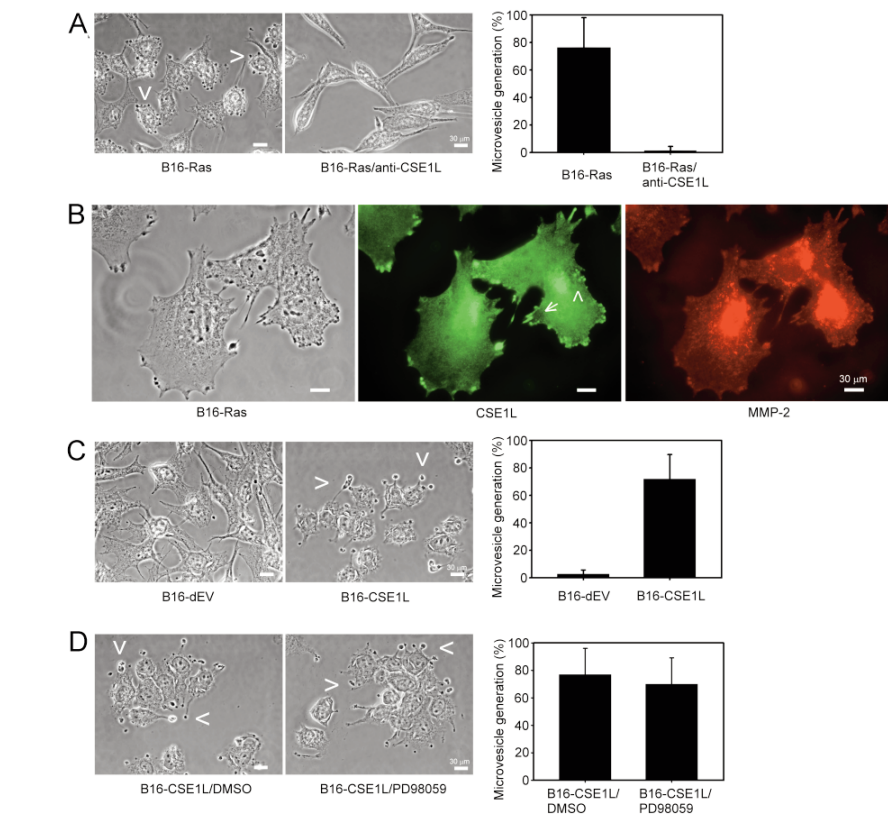


Figure 2. CSE1L mediates microvesicle biogenesis induced by v-H-ras. (A) Representative micrographs show that CSE1L knockdown inhibited v-H-Ras-induced microvesicle biogenesis. (B) Immunofluorescence shows CSE1L and MMP-2 staining in microvesicles in the cytoplasm (arrowhead) and the base of invadopodia (arrow) of B16-Ras cells. (C) Representative images show CSE1L overexpression stimulates microvesicle generation in B16-CSE1L cells. (D) Representative micrograph of B16-CSE1L cells treated with DMSO or PD98059 in medium without FBS for 12 h.

jected with viable cells (3×10^4 cells in 100 μL PBS/mouse) in the tail vein. The experiment included 11, 14, 8 and 11 mice injected with B16-dEV, B16-CSE1L, B16-Ras and B16-Ras/anti-CSE1L cells, respectively. Three weeks after injection, the mice were sacrificed and necropsied. The numbers of tumors in lungs were counted by macrography and micrography. Mouse care and experimental procedures were performed following the guidelines of the Animal Care Committee of Academia Sinica (Taiwan). There were 3, 10, 4 and 1 mice that died 3 wks after being injected with B16-dEV, B16-CSE1L, B16-Ras and B16-Ras/anti-CSE1L cells, respectively, and thus these mice were excluded from the statistics. There were 1, 1, 0 and 3 mice injected with B16-

dEV, B16-CSE1L, B16-Ras and B16-Ras/anti-CSE1L cells, respectively, that did not grow tumors in the lungs and thus were also excluded from the statistics.

Immunogold Electron Microscopy

Cells grown on Aclar film (Electron Microscopy Sciences, Hatfield, PA, USA) were washed with PBS and fixed in a mixture of 0.5% glutaraldehyde and 2% paraformaldehyde in HEPES buffer (pH 6.8) for 15 min and were then placed in 2% paraformaldehyde in HEPES buffer (pH 6.8) at 4°C for 14 d. Samples were dehydrated with 80% ethanol and infiltrated with increasing concentrations of Lowicryl HM20 resin (Polysciences, Tokyo, Japan). Polymerization of Lowicryl HM20 was performed by ultraviolet irra-

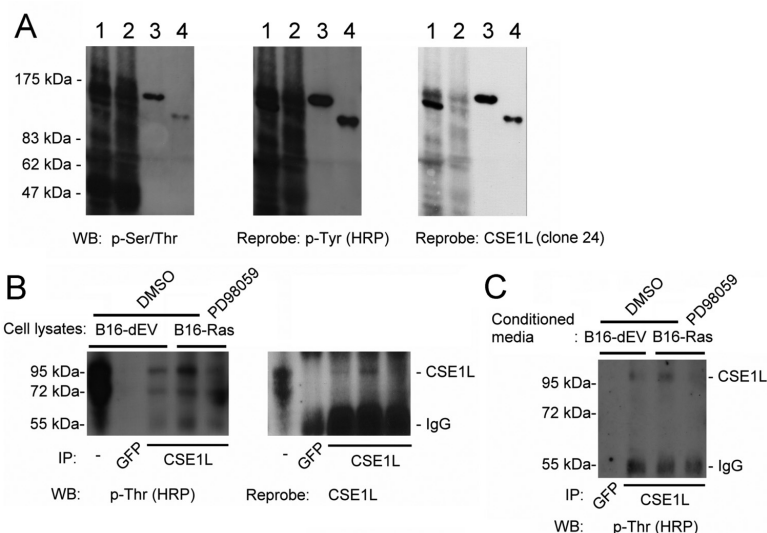


Figure 3. v-H-ras induces ERK-dependent CSE1L phosphorylation and secretion. (A) Immunoblot analysis of CSE1L phosphorylation with synthesized CSE1L protein produced by wheat germ cell-free protein synthesis system. Lane 1: B16-dEV cell lysate; lane 2: CSE1L-depleted cell lysates produced by depleting CSE1L with anti-CSE1L antibodies and A/G plus agarose; lane 3: recombinant GST-CSE1L protein; lane 4: CSE1L protein. (B) Levels of threonine-phosphorylated CSE1L in B16-dEV and B16-Ras cells treated with DMSO or PD98059 for 24 h. The levels were analyzed by immunoprecipitation of the samples with anti-CSE1L antibodies and immunoblotting with HRP-conjugated anti-phosphothreonine antibodies. The immunoblot was reprobated with anti-CSE1L antibodies. Control immunoprecipitation was performed by using mouse anti-GFP antibodies. (C) Levels of secretory threonine-phosphorylated CSE1L in cell number-standardized conditioned media harvested from serum-starved B16-dEV and B16-Ras cells treated with DMSO or PD98059 for 24 h. The levels were analyzed by immunoprecipitation of the samples with anti-CSE1L antibodies and immunoblotting with HRP-conjugated anti-phosphothreonine antibodies.

diation (wavelength peak at 360 nm) for 24 h. Ultrathin sections were cut and then mounted on nickel grids coated with 2% Neoprene (Ohken, Tokyo, Japan). After being sunk in 100% ethanol for 3 min, samples were immersed in 0.01 mol/L EDTA (pH 7.2) at 65°C for 24 h. The samples were washed with PBS three times (5 min/wash) and blocked with PBS containing 1% BSA and 0.1% Tween-20 for 15 min. The samples were incubated with a mixture of primary antibodies (CSE1L, clone 3D8) diluted in PBS (1:20) for 1 h, washed with PBS three times (5 min/wash) and reacted with 12-nm gold-labeled secondary antibodies, followed by washing with PBS three times (5 min/wash). The samples were stained with uranyl acetate and were examined on a Hitachi H-7000 transmission electron microscope (Hitachi, Tokyo, Japan).

Preparation of Microvesicles

Microvesicles were prepared from conditioned media by size exclusion chromatography and ultracentrifugation. Briefly, conditioned media were applied to a Sepharose 2B column (Amersham Biosciences, Piscataway, NJ, USA) equilibrated with PBS. Fractions (1 mL) were collected, and the protein content was monitored by measuring absorbance at 280 nm. The void volume peak material, containing proteins of >50 million kDa, was then centrifuged at 16,000g for 1 h at 4°C. The pellet contains microvesicles and was resuspended with 50 μL PBS.

For labeling of microvesicles isolated from cancer sera, the cancer sera were made free of platelets and cellular debris by centrifuging at 2,500g for 20 min two times. The supernatant was then centrifuged at 16,000g for 1 h in 4°C to pre-

cipitate microvesicles. The pellet was washed with and resuspended in PBS. The microvesicles were incubated with a mixture of primary antibodies (CSE1L, clone H2) diluted in PBS (1:100) for 1 h and followed by incubating with secondary antibodies coupled to Alexa Fluor 568. Control immunofluorescence was performed with the samples stained with Alexa Fluor 568-labeled secondary antibodies. The samples were examined with an inverted fluorescence microscope.

In Vivo Tumor Imaging

Anti-CSE1L antibodies (clone 24) and anti-mouse IgG were conjugated with quantum dots by using a Qdot 800 Antibody Conjugation Kit (Invitrogen) according to the manufacturer's instructions. Briefly, Qdots were activated with N-succinimidyl 4-(N-maleimidomethyl) cyclohexane-1-carboxylate (SMCC), and the antibodies were reduced by dithiothreitol. The reduced antibodies were covalently coupled with activated Qdots, and the conjugation reactions were quenched with β-mercaptoethanol. Conjugates were concentrated by ultrafiltration and purified by size exclusion chromatography. The concentrations of conjugates were determined with a spectrofluorometer.

Male C57BL/6 mice aged between 6 and 7 wks were injected with viable B16-CSE1L cells (3×10^4 cells in 100 μL PBS/mouse) in the dorsal skin. Three weeks after tumor inoculation, mice bearing tumors were injected with quantum dots conjugated with anti-CSE1L antibodies or anti-mouse IgG (500 pmol in 100 μL PBS/mouse) into the tail vein. Mice were imaged by using a Xenogen IVIS 200 imaging system (excitation: 525/50 nm; emission: 832/65 nm) at 0, 1 and 4 h after injection. The near-infrared fluorescence images were processed under the same conditions and acquired on a camera.

Statistical Analysis

Data were analyzed by using SPSS 12.0 statistical software (SPSS, Chicago, IL, USA). Statistical differences were analyzed by a paired *t* test. An α level of

0.05 was used to determine statistical significance.

All supplementary materials are available online at www.molmed.org.

RESULTS

v-H-ras Expression Triggers Microvesicle Biogenesis

The C57BL/6 mouse strain is a frequently used animal model for studying cancer development, and B16F10 melanoma cells have been shown to be a highly metastatic cancer cell line in C57BL/6 mice (32). B16F10 cells were transfected with the control vectors and v-H-ras-expressing vectors to obtain B16-dEV and B16-Ras cells, respectively (Supplementary Figure S1). Microscopic examination showed the surfaces of B16-Ras cells were decorated with many bubble-like microvesicles, and this was not observed in the B16-dEV control cells (Figure 1A). Formation of microvesicles is often coupled with the extension of cell pseudopodia (33). Developing microvesicles were observed in the pseudopodia and cytoplasm of B16-Ras cells (Figure 1B). Treatment with the ERK inhibitor PD98059 inhibited v-H-ras-induced phosphorylation/activation of ERK and inhibited v-H-ras-induced microvesicle biogenesis (Figures 1C, D). Microvesicles are rich in extracellular proteases, which are essential for tumor metastasis (12). MMP-2 is an extracellular protease that plays an important role in the progression of various diseases including tumor metastasis (34–37). Immunofluorescence showed that microvesicles produced by B16-Ras cells were rich in MMP-2 (Supplementary Figure S2A). We isolated microvesicles from the conditioned media of the cells, and the results of immunoblotting showed v-H-ras transfection increased microvesicular MMP-2 level in an ERK-dependent manner (Supplementary Figure S2B). There was no accumulation of microvesicles in the surface of PD98059-treated B16-Ras cells due to inhibition of microvesicle shedding by ERK repression

(Figure 1D). Thus, v-H-ras regulates microvesicle biogenesis in an ERK-dependent manner.

CSE1L Mediates Microvesicle Generation Triggered by v-H-ras

CSE1L has been shown to regulate the secretion of MMP-2 and promote the invasion of tumor cells (38–40). We investigated whether CSE1L was involved in microvesicle biogenesis and MMP-2 secretion induced by Ras. Knockout of the *cse1l* gene has been shown to be embryonically lethal in mice (41). Therefore, we knock down CSE1L expression to study the effect of CSE1L on microvesicle generation induced by v-H-Ras. B16-Ras cells were transfected with the *cse1l*-specific shRNA-expressing vectors to obtain the B16-Ras/anti-CSE1L cells (Supplementary Figure S1). Microscopic examination showed there was no microvesicle present in the surfaces of B16-Ras/anti-CSE1L cells (Figure 2A). Immunofluorescence showed CSE1L was located in both the nuclei and the cytoplasm of cells, and in the cytoplasm, CSE1L was preferentially accumulated in developing microvesicles that were located in the invadopodia of B16-Ras cells (Figure 2B). Thus, we studied whether CSE1L stimulated microvesicle biogenesis. B16F10 cells were transfected with CSE1L-expressing vectors to obtain the B16-CSE1L cells (Supplementary Figure S1). CSE1L is known to regulate invadopodia extension of cells (29). Microscopic examination showed the presence of microvesicles in the tips of invadopodia in B16-CSE1L cells (Figure 2C). CSE1L also stimulated microvesicle generation in MCF-7 cells and HT-29 cells (data not shown). PD98059 treatment was unable to inhibit microvesicle generation induced by CSE1L (Figure 2D). These results indicate that CSE1L mediates the biogenesis of microvesicles.

v-H-ras Induces ERK-Dependent Threonine Phosphorylation and Secretion of CSE1L

We studied the expression of phosphorylated ERK and CSE1L in colorectal cancer. The

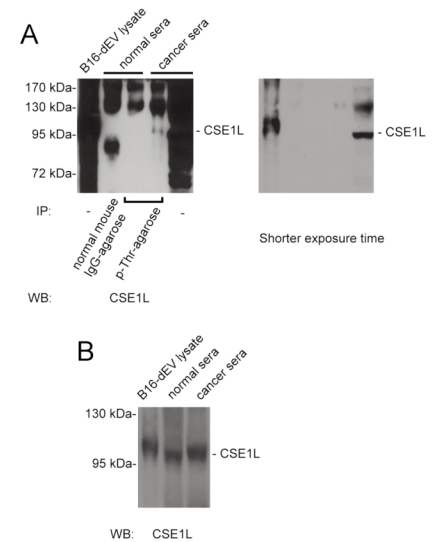


Figure 4. Presence of phosphorylated CSE1L in sera from cancer patients. (A) Serum threonine-phosphorylated CSE1L analyzed by immunoprecipitation with agarose-conjugated anti-phosphothreonine antibodies and a pool of sera from 36 colorectal cancer patients (each 10 μ L) or 36 healthy donors (each 10 μ L) and immunoblotting with anti-CSE1L antibodies. Control immunoprecipitation was performed using agarose-conjugated normal mouse IgG. (B) The levels of CSE1L in the pools of cancer sera ($n = 36$) and normal sera ($n = 36$) were analyzed by immunoblotting with anti-CSE1L antibodies (clone 24).

anti-CSE1L antibody (clone 24) was strong for immunofluorescence, immunoblotting and immunoprecipitation; but its immunoreactivity was weak for paraffin-embedded tissue. Immunohistochemical analyses of paraffin-embedded tissue microarray with anti-ERK (MK1) and anti-CSE1L (clone 3D8) antibodies showed significant expression of phospho-ERK (100%, 115/115) and CSE1L (99.1%, 114/115) in colorectal cancer (Supplementary Figure S3A). The margin of normal tissue only showed weak phospho-ERK and CSE1L expression (Supplementary Figure S3A). Moreover, there was a coincidence in the relative staining intensity of CSE1L with phospho-ERK in the tumor (97.4%, 112/115) (Supplementary Figure S3B), indicating

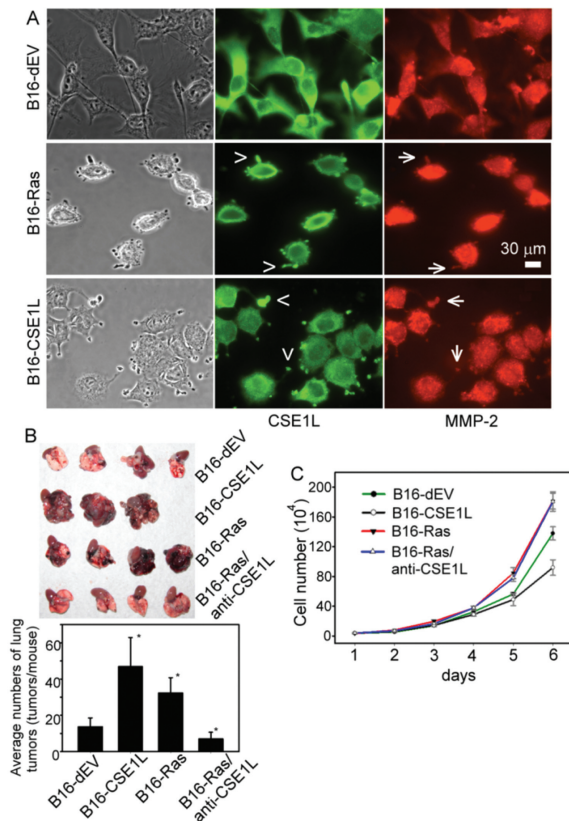


Figure 5. CSE1L mediates metastasis of tumor cells induced by v-H-ras. (A) Representative images show colocalization of CSE1L (arrowheads) with MMP-2 (arrows) in microvesicles analyzed by immunofluorescence with anti-CSE1L and anti-MMP-2 antibodies. (B) Animal models showed CSE1L mediated metastasis of B16F10 melanoma cells induced by v-H-ras. Upper half is a representative photograph of the pulmonary tumors of C57BL/6 mice injected with B16-dEV, B16-CSE1L, B16-Ras and B16-Ras/anti-CSE1L cells. $P = 0.06$ between mice injected with B16-CSE1L and B16-dEV cells. $P = 0.03$ between mice injected with B16-Ras and B16-dEV cells. $P = 0.02$ between mice injected with B16-Ras/anti-CSE1L and B16-dEV cells. $P = 0.01$ between mice injected with B16-Ras and B16-Ras/anti-CSE1L cells. (C) Growth curves of B16-dEV, B16-CSE1L, B16-Ras and B16-Ras/anti-CSE1L cells. The graph represents the results of three independent assays.

that there was a close relationship between ERK and CSE1L in colorectal cancer progression. Immunohistochemical analysis also showed that CSE1L and phospho-ERK were highly expressed in human breast tumors and melanoma (Supplementary Figure S3C). Coincidences in the relative staining intensity of CSE1L with phospho-ERK in the tumor were also observed in breast cancer and melanoma (Supplementary Figure S3C).

Immunoblotting with GST-CSE1L fusion protein produced by wheat germ cell-free protein synthesis system showed

CSE1L reacted with anti-phosphoserine/threonine and anti-phosphotyrosine antibodies (Figure 3A). The result of immunoprecipitation showed that v-H-ras expression increased the phosphorylation of CSE1L, and PD98059 treatment inhibited v-H-ras–increased phosphorylation of CSE1L (Figure 3B). The results of immunoprecipitation with the cell number–standardized conditioned media also showed that v-H-ras expression increased the secretion of phosphorylated CSE1L, and PD98059 treatment inhibited v-H-ras–induced secretion of phosphorylated CSE1L (Figure 3C). Thus, v-H-ras induces

ERK-dependent phosphorylation and secretion of CSE1L.

Presence of Phosphorylated CSE1L in Sera from Cancer Patients

We analyzed the presence of phosphorylated CSE1L in sera from cancer patients. Immunoprecipitation with sera from patients with colorectal cancer ($n = 36$) and from the healthy donors ($n = 36$) showed the presence of a dense phosphorylated CSE1L protein band around 100 kDa in the immunoblots of anti-phosphothreonine antibody–reacted immunoprecipitates in sera from cancer patients, and no CSE1L protein band was observed in the immunoblots of the normal serum samples (Figure 4A). Although the serum CSE1L level was higher in cancer serum samples than in healthy donor serum samples, the difference was not as significant as that observed in the assay of phosphorylated CSE1L (Figure 4B). Therefore, serum phosphorylated CSE1L may be a potential biomarker for cancer diagnosis.

CSE1L Mediates the Metastasis of Tumor Cells Induced by v-H-ras

The proteolytic activities of microvesicles play an important role in tumor metastasis (13). Immunofluorescence showed CSE1L was colocalized with MMP-2 in microvesicles (Figure 5A). We isolated microvesicles from the conditioned media of the cells. Gelatin zymography assay showed v-H-ras expression increased the microvesicular MMP-2 zymographic activity, and PD98059 treatment attenuated the v-H-ras–induced increase in microvesicular MMP-2 zymographic activity in B16F10 cells (Supplementary Figure S4A). CSE1L knockdown also attenuated the v-H-ras–induced increase in microvesicular MMP-2 zymographic activity (Supplementary Figure S4A). Immunofluorescence also showed that CSE1L was colocalized with MMP-9 in microvesicles (Supplementary Figure S4B). Gelatin zymography assay showed v-H-ras expression increased the microvesicular MMP-9 zymographic activity, and CSE1L knock-

down attenuated the v-H-ras-induced increase in microvesicular MMP-9 zymographic activity (Supplementary Figure S4C). Matrigel-based invasion assay showed that both v-H-Ras and CSE1L enhanced the *in vitro* invasion of B16F10 cells, and CSE1L knockdown attenuated the v-H-Ras-induced increase in the invasion of B16F10 cells (Supplementary Figure S4D). Animal metastasis models showed v-H-Ras expression increased the pulmonary metastasis of B16F10 cells by 246.1% ($P = 0.03$) in C57BL/6 mice, and CSE1L knockdown attenuated the v-H-Ras-induced increase in the tumor pulmonary metastasis of the cells by 100% ($P = 0.01$); although, the growth rates of B16-Ras and B16-Ras/anti-CSE1L cells were similar (Figures 5B, C). The mean \pm standard deviation of lung tumors were 13.7 ± 4.8 , 47 ± 15.8 , 32.2 ± 8.5 and 7 ± 3.6 tumors per mouse for mice injected with B16-dEV, B16-CSE1L, B16-Ras and B16-Ras/anti-CSE1L cells, respectively. CSE1L overexpression also increased the mortality of mice injected with B16-F10 cells; there were 3, 10, 4 and 1 mice that died 3 wks after injection with B16-dEV, B16-CSE1L, B16-Ras and B16-Ras/anti-CSE1L cells, respectively. Thus, CSE1L mediates the metastasis of tumor cells induced by v-H-Ras.

CSE1L Is a Microvesicle Membrane Protein and Anti-CSE1L Antibodies Can Target Tumors

We studied the distribution of CSE1L in microvesicles. Immunofluorescence showed CSE1L was preferentially accumulated in microvesicles; although MMP-2 was also located in microvesicles, no preferential accumulation of MMP-2 in microvesicles was observed (Figure 6A). The results of immunofluorescence also showed that CSE1L was located in the membranes of microvesicles (Figure 6B). Immunogold electron microscopy showed that CSE1L (12-nm gold, arrowheads) was located in the membranes of microvesicles and also in the dense-stained material within microvesicles (Figure 6C). We isolated microvesicles from the sera of colorectal cancer

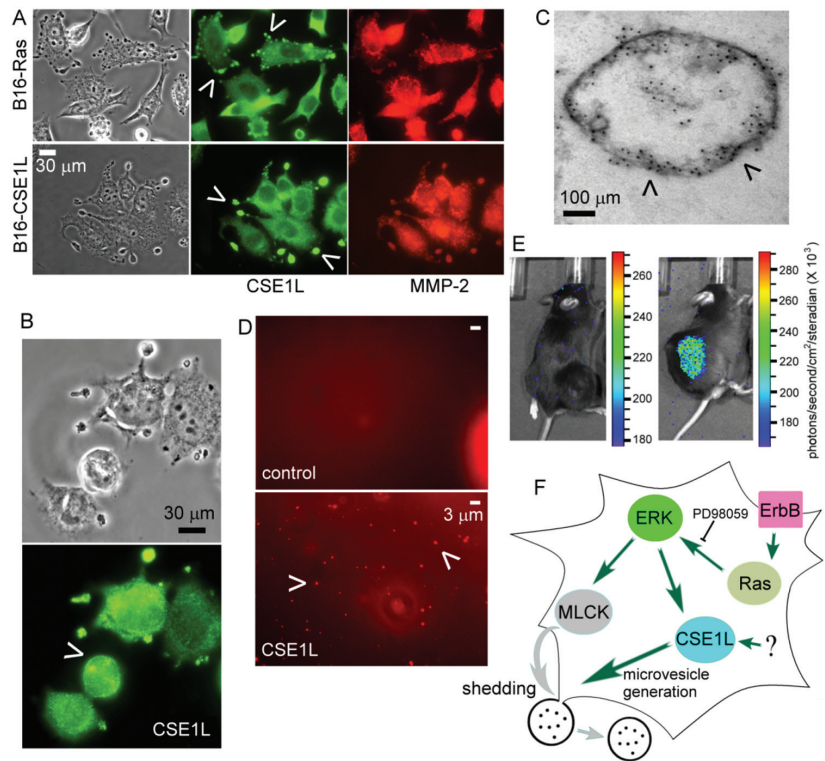


Figure 6. CSE1L is a microvesicle membrane protein and anti-CSE1L antibodies can target tumors. (A) Representative immunofluorescence show preferential accumulation of CSE1L (arrowheads) in microvesicles. MMP-2 distribution was analyzed for comparison. (B) Localization of CSE1L in microvesicle membranes (arrowhead) analyzed by immunofluorescence. (C) A representative immunogold electron microscopic image shows CSE1L (12-nm gold, arrowheads) distributions in microvesicle in B16-Ras cells. (D) Representative immunofluorescence shows CSE1L (arrowheads) staining in microvesicles harvested from the sera of colorectal cancer patients. Control immunofluorescence was performed with the samples stained with secondary antibodies coupled with Alexa 568 (lower panel). (E) Representative images show near-infrared fluorescence signals of mice bearing B16-CSE1L cell-derived tumors injected with Qdot-conjugated anti-CSE1L antibodies (right, $n = 3$) or Qdot-conjugated anti-mouse IgG (left, $n = 3$) at 4 h after injection. (F) Pathway of Ras-ERK-CSE1L signaling in the regulation of microvesicle biogenesis. Ras activated by the upstream signaling such as the ErbB2 results in ERK activation. ERK interacts with CSE1L, which in turn mediates microvesicle biogenesis. CSE1L-induced microvesicle biogenesis is not inhibited by PD98059, indicating that there is a signaling pathway other than ERK that also interacts with CSE1L and regulates microvesicle generation. ERK activation also results in MLCK activation, which in turn modulates microvesicle shedding.

patients. The results of immunofluorescence showed positive staining of CSE1L in the microvesicles harvested from the cancer sera (Figure 6D). The shed microvesicles may remain in the extracellular environment around tumor cells. Therefore, localization of CSE1L in the membranes of microvesicles indicates that CSE1L may be a therapeutic target for cancer. C57BL/6 mice bearing tumors

were injected with quantum dots conjugated with anti-CSE1L antibodies or anti-mouse IgG as the control in the tail vein. The results of *in vivo* imaging showed the presence of significant near-infrared fluorescence signal in tumors of mice injected with the anti-CSE1L antibody-conjugated quantum dots but not in tumors of mice injected with the control IgG-conjugated quantum dots (Fig-

ure 6E). Therefore, CSE1L is a potential target for cancer therapy.

DISCUSSION

Microvesicles play important roles in normal physiological functions as well as the cellular processes that lead to the pathogenesis of various diseases (1–6). Ras may activate a second signaling pathway that involves the Ras-related protein RhoA (42). Li *et al.* (43) reported that RhoA triggers a specific signaling pathway that generates microvesicles in cancer cells. We showed that the Ras-ERK pathway mediated microvesicle biogenesis and metastasis of tumor cells. Both studies demonstrate that Ras signaling plays a key role in regulating microvesicle biogenesis and consequently the malignant progression of the tumor. We further showed that CSE1L is a microvesicle membrane protein that mediates microvesicle generation triggered by Ras. The proposed pathway of Ras-ERK-CSE1L signaling in the regulation of microvesicles biogenesis is outlined (Figure 6F). The Ras-ERK signaling is a major pathway downstream in the erythroblastic leukemia viral oncogene homolog/human epidermal growth factor receptor (ErbB/HER) family, an important target for targeted cancer therapy (44,45). CSE1L is linked to Ras-ERK signaling, and phosphorylated CSE1L is present in the serum of cancer patients (Figure 4). Therefore, serum phosphorylated CSE1L may be a potential marker for cancer diagnosis as well as for monitoring the response of targeted therapy in HER/ErbB-positive cancer.

We showed that CSE1L was located in microvesicles and regulated the biogenesis of microvesicles (Figure 2). Unlike microvesicles induced by v-H-ras, CSE1L induced larger sizes but fewer numbers of microvesicles per cell (Figure 2C). The differences are reasonable, since CSE1L-induced microvesicles were mainly present in the tips of invadopodia; thus, microvesicles accumulated in the tips of invadopodia and became bigger in size. Also, CSE1L was located in the micro-

vesicle membrane, and the dense stained material within microvesicles (Figure 6C). Therefore, CSE1L may play a role in maintaining the structural integrity of the microvesicle compartment; this might also contribute to the larger size of microvesicles induced by CSE1L. CSE1L is a multifunctional protein and is implicated in microtubule assembly (19,29), nuclear transport (46), transcriptional regulation (47), apoptosis (48,49) and cancer invasion and metastasis (26). Associations of CSE1L with microtubules, nuclear transporter factor and chromosomes have been reported before (19,29,46,47). These facts suggest that the cellular pool of CSE1L protein must be delicately regulated. Further study of the extracellular stimuli, including the tumor microenvironment, and the cellular signaling that regulates the cellular distribution and association of CSE1L with other protein is needed to illustrate the physiological/pathological functions of CSE1L.

CSE1L was recently investigated in a larger series of colorectal cancers, and its association with regulation of MMP-9 was also studied (50). Our results also showed that CSE1L was colocalized with MMP-9 in microvesicles and regulated Ras-induced zymographic activity of MMP-9 (Supplementary Figures S4B, S4C). Ras signaling is known to play a critical role in MMP-2 and MMP-9 secretion and, subsequently, in the invasiveness of tumor cells (51,52). We showed that Ras-stimulated MMP-2 and MMP-9 secretion through the regulation of microvesicle generation and CSE1L mediated microvesicle generation triggered by Ras. Because MMP-2 and MMP-9 play important roles in tumor metastasis, these findings may offer an approach for blocking MMP-2 and MMP-9 secretion for the inhibition of tumor metastasis. Microvesicles can deliver mRNA, miRNA and bioactive proteins between cells and play an essential role in regulating intercellular communication in the pathological processes of various diseases (1–6). Therefore, these findings may also offer an approach for regulat-

ing microvesicle biogenesis for the control of disease progression.

The accumulated results have suggested that the metastasis of tumor cells from a primary tumor mass can occur “early” and “late” in tumorigenesis (7,53). In the late metastasis, the accumulation of aberrations in tumor cells makes the tumor cells acquire aggressive phenotypes and metastasize to ectopic sites in the hosts. In the early metastasis, oncogenes and tumor suppressor genes that associated with tumor initiation and proliferation can, at a much earlier than previously recognized stage in the tumor’s evolution, promote metastasis (7,54). The tumor microenvironment such as the extracellular matrix surrounding tumor cells acts as a barrier to invasion and migration, and MMP-2 and MMP-9 play important roles in extracellular matrix degradation and metastatic tumor progression (12,34,35). Ras is associated with both the initiation and malignant progression of the tumor (9,10,44,45). We showed that CSE1L mediated Ras-triggered microvesicle generation and metastasis of tumor cells (Figure 5). Furthermore, CSE1L was colocalized with MMP-2 and MMP-9 in microvesicles and regulated the Ras-induced increase in MMP-2 and MMP-9 zymographic activities (Supplementary Figure S4). MMP-2 and MMP-9 are implicated in both the early and late metastasis of tumor cells in tumorigenesis (7). It was also reported that early-stage colorectal cancer patients whose tumors showed strong CSE1L cytoplasmic expression had a worse survival outcome (50). Taken together, these findings indicate that CSE1L may play important roles in both the early and late metastasis of tumor in tumor tumorigenesis.

We showed the presence of phosphorylated CSE1L in the sera of the colorectal cancer patients, and phosphorylated CSE1L was hard to be detected in the sera of the healthy donors (Figure 4). Although the study included only a limited number of samples ($n = 36$ in each group), it did show the presence of the phosphorylated CSE1L protein in

the sera of patients with the colorectal cancer and its absence in the sera of healthy controls. We used immunoprecipitation to examine the presence of phosphorylated CSE1L in the sera of cancer patients. Although this technique could detect the presence of phosphorylated CSE1L directly on the blots, there is a need to develop a technique for analyzing the clinical-pathological correlation between serum phosphorylated CSE1L and cancer in a large cohort study.

A significant limitation in targeted cancer therapy is that not all patients can receive targeted therapy, since the patient's tumor may be "target-negative." Also, tumor-related mortalities may still occur in targeted therapy because of the proliferation of the target-negative tumor cells. Cancer patients have an increased level of circulating microvesicles (55). Tumor cells constitutionally release microvesicles, and thus there may be a relatively higher level of microvesicles in the tumor microenvironment (4,30). Hence, microvesicle membrane proteins may be the potential targets for cancer treatment. Actually, a few patents concerning vesicles and their use in cancer chemotherapy have already been delivered (56). CSE1L is highly expressed in cancer (20–28). We showed that CSE1L was preferentially accumulated in microvesicles and it is a microvesicle membrane protein (Figure 6). Therefore, CSE1L may be a potential target for the development of targeted therapy for most cancer patients.

CONCLUSION

The findings that CSE1L mediates Ras-triggered microvesicle generation and metastasis of tumor cells highlight a novel role of Ras signaling in tumor progression. Serum phosphorylated CSE1L may be a potential marker for cancer diagnosis as well as for monitoring the response of targeted therapy in HER/ErBB-positive cancer. Furthermore, CSE1L is a microvesicle membrane protein, and it may be a potential target for cancer therapy.

ACKNOWLEDGMENTS

This study was supported by a grant from the National Science Council (NSC 101-2314-B-038-038).

DISCLOSURE

Patents regarding microvesicle detection and phosphorylated CSE1L are in applications.

REFERENCES

- Cocucci E, Racchetti G, Meldolesi J. (2009) Shedding microvesicles: artefacts no more. *Trends Cell Biol.* 19:43–51.
- Sidhu SS, Mengistab AT, Tauscher AN, LaVail J, Basbaum C. (2004) The microvesicle as a vehicle for EMMPRIN in tumor-stromal interactions. *Oncogene.* 23:956–63.
- Ratajczak J, Wysoczynski M, Hayek F, Janowska-Wieczorek A, Ratajczak MZ. (2006) Membrane-derived microvesicles: important and underappreciated mediators of cell-to-cell communication. *Leukemia.* 20:1487–95.
- Skog J, et al. (2008) Glioblastoma microvesicles transport RNA and proteins that promote tumor growth and provide diagnostic biomarkers. *Nat. Cell Biol.* 10:1470–6.
- Svensson KJ, et al. (2011) Hypoxia triggers a proangiogenic pathway involving cancer cell microvesicles and PAR-2-mediated heparin-binding EGF signaling in endothelial cells. *Proc. Natl. Acad. Sci. U. S. A.* 108:13147–52.
- Wang H, et al. (2012) Oxidized low-density lipoprotein-dependent platelet-derived microvesicles trigger procoagulant effects and amplify oxidative stress. *Mol. Med.* 18:159–66.
- Coghlin C, Murray GI. (2010) Current and emerging concepts in tumour metastasis. *J. Pathol.* 222:1–15.
- Dolo V, Ginestra A, Ghersi G, Nagase H, Vittoelli ML. (1994) Human breast carcinoma cells cultured in the presence of serum shed membrane vesicles rich in gelatinolytic activities. *J. Submicrosc. Cytol. Pathol.* 26:173–80.
- Dolo V, Adobati E, Canevari S, Picone MA, Vittoelli ML. (1995) Membrane vesicles shed into the extracellular medium by human breast carcinoma cells carry tumor-associated surface antigens. *Clin. Exp. Metastasis.* 13:277–86.
- Giusti I, et al. (2008) Cathepsin B mediates the pH-dependent proinvasive activity of tumor-shed microvesicles. *Neoplasia.* 10:481–8.
- Wysoczynski M, Ratajczak MZ. (2009) Lung cancer secreted microvesicles: underappreciated modulators of microenvironment in expanding tumors. *Int. J. Cancer.* 125:1595–603.
- Doeuvre L, Angles-Cano E. (2009) Cell-derived microparticles unveil their fibrinolytic and proteolytic function. *Med. Sci. (Paris).* 25:37–44.
- Dolo V, et al. (1999) Matrix-degrading proteinases are shed in membrane vesicles by ovarian cancer

cells in vivo and in vitro. *Clin. Exp. Metastasis.* 17:131–40.

- Bos JL. (1989) ras oncogenes in human cancer: a review. *Cancer Res.* 49:4682–9.
- Yoakum GH, et al. (1985) Transformation of human bronchial epithelial cells transfected by Harvey ras oncogene. *Science.* 227:1174–9.
- Thorgeirsson UP, et al. (1985) NIH/3T3 cells transfected with human tumor DNA containing activated ras oncogenes express the metastatic phenotype in nude mice. *Mol. Cell Biol.* 5:259–62.
- Pylayeva-Gupta Y, Grabocka E, Bar-Sagi D. (2011) RAS oncogenes: weaving a tumorigenic web. *Nat. Rev. Cancer.* 11:761–74.
- Muralidharan-Chari V, et al. (2009) ARF6-regulated shedding of tumor cell-derived plasma membrane microvesicles. *Curr. Biol.* 19:1875–85.
- Brinkmann U, Brinkmann E, Gallo M, Pastan I. (1995) Cloning and characterization of a cellular apoptosis susceptibility gene, the human homologue to the yeast chromosome segregation gene CSE1. *Proc. Natl. Acad. Sci. U. S. A.* 92:10427–31.
- Wellmann A, et al. (1997) Localization of the cell proliferation and apoptosis-associated CAS protein in lymphoid neoplasms. *Am. J. Pathol.* 150:25–30.
- Böni R, Wellmann A, Man YG, Hofbauer G, Brinkmann U. (1999) Expression of the proliferation and apoptosis-associated CAS protein in benign and malignant cutaneous melanocytic lesions. *Am. J. Dermatopathol.* 21:125–8.
- Peiro G, Diebold J, Lohrs U. (2002) CAS (cellular apoptosis susceptibility) gene expression in ovarian carcinoma: correlation with 20q13.2 copy number and cyclin D1, p53, and Rb protein expression. *Am. J. Clin. Pathol.* 118:922–9.
- Ouellet V, et al. (2006) Tissue array analysis of expression microarray candidates identifies markers associated with tumor grade and outcome in serous epithelial ovarian cancer. *Int. J. Cancer.* 119:599–607.
- Behrens P, Brinkmann U, Fogt F, Wernert N, Wellmann A. (2001) Implication of the proliferation and apoptosis associated CASL/CAS gene for breast cancer development. *Anticancer Res.* 21:2413–7.
- Uen WC, et al. (2010) Differential distributions of CSE1L/CAS and E-cadherin in the polarized and non-polarized epithelial glands of neoplastic colorectal epithelium. *J. Mol. Histol.* 41:259–66.
- Tai CJ, Chang CC, Shen SC, Lee WR, Jiang MC. (2011) Serum cellular apoptosis susceptibility (CSE1L/CAS) protein for cancer diagnosis. *J. Exp. Clin. Med.* 3:104–7.
- Chang CC, et al. (2012) The prognostic significance of nuclear CSE1L in urinary bladder urothelial carcinomas. *Ann. Diagn. Pathol.* 16:362–8.
- Tai CJ, et al. (2012) Presence of CSE1L protein in urine of patients with urinary bladder urothelial carcinomas. *Int. J. Biol. Markers.* 27:e280–4.
- Tai CJ, et al. (2010) Increased cellular apoptosis susceptibility (CSE1L/CAS) protein expression promotes protrusion extension and enhances mi-

- gration of MCF-7 breast cancer cells. *Exp. Cell Res.* 316:2969–81.
30. Ratajczak J, Wysoczynski M, Hayek F, Janowska-Wieczorek A, Ratajczak MZ. (2006) Membrane-derived microvesicles: important and underappreciated mediators of cell-to-cell communication. *Leukemia.* 20:1487–95.
 31. Liu JJ, *et al.* (1995) Ras transformation results in an elevated level of cyclin D1 and acceleration of G1 progression in NIH 3T3 cells. *Mol. Cell Biol.* 15:3654–63.
 32. Qian H, *et al.* (2007) RNA interference of metastasis-associated gene 1 inhibits metastasis of B16F10 melanoma cells in a C57BL/6 mouse model. *Biol. Cell.* 99:573–81.
 33. Bianco F, *et al.* (2005) Astrocyte-derived ATP induces vesicle shedding and IL-1 beta release from microglia. *J. Immunol.* 174:7268–77.
 34. Emmert-Buck MR, *et al.* (1994) Increased gelatinase A (MMP-2) and cathepsin B activity in invasive tumor regions of human colon cancer samples. *Am. J. Pathol.* 145:1285–90.
 35. Zitta K, *et al.* (2012) Serum from patients undergoing remote ischemic preconditioning protects cultured human intestinal cells from hypoxia-induced damage: involvement of matrix metalloproteinase-2 and -9. *Mol. Med.* 18:29–37.
 36. Atif F, *et al.* (2011) Progesterone inhibits the growth of human neuroblastoma: in vitro and in vivo evidence. *Mol. Med.* 17:1084–94.
 37. Brik R, *et al.* (2010) Salivary antioxidants and metalloproteinases in juvenile idiopathic arthritis. *Mol. Med.* 16:122–8.
 38. Liao CF, *et al.* (2008) CSE1L/CAS, the cellular apoptosis susceptibility protein, enhances invasion and metastasis but not proliferation of cancer cells. *J. Exp. Clin. Cancer Res.* 27:15.
 39. Tung MC, *et al.* (2009) Higher prevalence of secretory CSE1L/CAS in sera of patients with metastatic cancer. *Cancer Epidemiol. Biomarkers Prev.* 18:1570–7.
 40. Stella Tsai CS, *et al.* (2010) Serum cellular apoptosis susceptibility protein is a potential prognostic marker for metastatic colorectal cancer. *Am. J. Pathol.* 176:1619–28.
 41. Bera TK, Bera J, Brinkmann U, Tessarollo L, Pastan I. (2001) Cse1l is essential for early embryonic growth and development. *Mol. Cell Biol.* 21:7020–4.
 42. Khosravi-Far R, Solski PA, Clark GJ, Kinch MS, Der CJ. (1995) Activation of Rac1, RhoA, and mitogen-activated protein kinases is required for Ras transformation. *Mol. Cell Biol.* 15:6443–53.
 43. Li B, Antonyak MA, Zhang J, Cerione RA. (2012) RhoA triggers a specific signaling pathway that generates transforming microvesicles in cancer cells. *Oncogene.* 2012, Jan 23. [Epub ahead of print].
 44. Downward J. (2003) Targeting RAS signalling pathways in cancer therapy. *Nat. Rev. Cancer* 3:11–22.
 45. Baines AT, Xu D, Der CJ. (2011) Inhibition of Ras for cancer treatment: the search continues. *Future Med. Chem.* 3:1787–808.
 46. Kutay U, Bischoff FR, Kostka S, Kraft R, Görlich D. (1997) Export of importin alpha from the nucleus is mediated by a specific nuclear transport factor. *Cell.* 90:1061–71.
 47. Tanaka T, Ohkubo S, Tatsuno I, Prives C. (2007) hCAS/CSE1L associates with chromatin and regulates expression of select p53 target genes. *Cell.* 130:638–50.
 48. Liao CF, *et al.* (2008) CSE1L/CAS, a microtubule-associated protein, inhibits taxol (paclitaxel)-induced apoptosis but enhances cancer cell apoptosis induced by various chemotherapeutic drugs. *BMB Rep.* 41:210–6.
 49. Liao CF, *et al.* (2008) CAS enhances chemotherapeutic drug-induced p53 accumulation and apoptosis: use of CAS for high-sensitivity anticancer drug screening. *Toxicol. Mech. Methods* 18:771–6.
 50. Alnabulsi A, *et al.* (2012) Cellular apoptosis susceptibility (chromosome segregation 1-like, CSE1L) gene is a key regulator of apoptosis, migration and invasion in colorectal cancer. *J. Pathol.* 2012, Mar 27 [Epub ahead of print].
 51. Liao J, Wolfman JC, Wolfman A. (2003) K-ras regulates the steady-state expression of matrix metalloproteinase 2 in fibroblasts. *J. Biol. Chem.* 278:31871–8.
 52. Gum R, *et al.* (1996) Stimulation of 92-kDa gelatinase B promoter activity by ras is mitogen-activated protein kinase kinase 1-independent and requires multiple transcription factor binding sites including closely spaced PEA3/ets and AP-1 sequences. *J. Biol. Chem.* 271:10672–80.
 53. Weinberg RA. (2008) Leaving home early: re-examination of the canonical models of tumour progression. *Cancer Cell.* 14:283–4.
 54. Klein CA. (2008) The metastatic cascade. *Science.* 321:1785–7.
 55. Castellana D, Toti F, Freyssinet JM. (2010) Membrane microvesicles: macromessengers in cancer disease and progression. *Thromb. Res.* 125:84–8.
 56. Wright PK. (2008) Targeting vesicle trafficking: an important approach to cancer chemotherapy. *Recent Pat. Anticancer Drug Discov.* 3:137–47.